2013 IEEE/ASME International Conference on
Advanced Intelligent Mechatronics (AIM)
Wollongong, Australia, July 9-12, 2013

Neural Controller for Swimming Modes and Gait Transition on an Ostraciiform Fish Robot

Wei Wang[1], Jiajie Guo[2], Zijian Wang[3] and Guangming Xie[1]

Abstract— **This paper proposes a novel control strategy with the central pattern generator (CPG) model for motion control of an ostraciiform fish robot. Compared with previous methods, this method can generate diverse swimming modes and manage gait transition with only two inputs. The CPG enables the robot to achieve agile swimming in the three-dimensional space and to automatically switch between the pectoral and caudal gaits with different speeds. Immediate application of the CPG model is illustrated on a boxfish robot propelled by two pectoral fins and one caudal fin, each of which is individually driven by a motor. With a vision sensor integrated in the CPG-based feedback control, the robot performs a target tracking behavior to further validate stability and availability of the model in real time. Both numerical simulation and laboratory experimental results are provided to validate the effectiveness of the proposed CPG model.**

I. Introduction

Inspired by the agility, efficiency and adaptivity of the animals, biomimetic robotics interacting with neuroscience has been an active research area with fruitful outcomes in the past decades. Using well-developed central nervous system and muscles/tendons, animals can smoothly modulate their locomotion (such as acceleration, deceleration, re-direction change and gait transition) with elegance and rapidity. By studying these excellent characteristics of animal motions, biomimetic robotics brings in innovative ideas to improve traditional robot designs [1], in terms of morphologies, locomotion models, control mechanisms and computational intelligence [2]. Designing locomotion control mechanism is a challenging task due to multiple redundancies, complicated biological models and smooth behavioral transitions in real time. The main problem of robots' locomotion control can be solved by central pattern generators (CPGs), which are neural networks capable of producing coordinated oscillatory patterns of rhythmic activity while receiving simple adjustment signals from higher control centers [3]. CPGs enable robots to continuously and smoothly modulate locomotion behaviors and gait transitions online. It is robust against transient perturbations with its limit cycle behaviors and can easily integrate sensory feedback into the coupled oscillation centers to improve adaptability [4].

Many CPG models have been widely applied to the swimming robots [5]–[9], most of which addressed anguilliform and carangiform swimming. The amphibious snake-like robots, AmphiBot I and II, fabricated and controlled by different CPG models, are able to smoothly swim under water and crawl on land [7]. A Hopf-based CPG model is implemented on an exhibition-oriented dolphin-like robot to demonstrate smooth transitions and well adaptation for 3D interactive swimming [10]. The CPG model is first applied to an ostraciiform swimming robot (Boxybot), which is capable of multiple swimming patterns in the 3D space [11].

It has been known that most fish perform obvious swimming gait transition as swimming speed increases [12], especially for the ostraciiform swimmers which acquire thrust by combinations of different fins. Several fish-like robots have successfully performed multiple swimming behaviors with the control of CPG models [6], [11], [13], [14]. However, these models need massive input parameters to control motion of the robot coordinately, and they do not address the problem that how the models are driven by command signals for gait generation and modulation on the fish-like robots. Based on our previous projects on the use of CPGs for controlling robotic fish [6], [14], [15], this paper proposes a numerical CPG model which uses only two parameters to emulate the ostraciiform swimming of its natural counterpart in the 3D space: one controls different swimming modes such as forward swimming, turning and rolling while another functions in swimming gait generation with different types of fins at different swimming speeds. The proposed model can be applied to all fish-like robots with paired and caudal fins.

In this paper, the CPG model duplicates most primary swimming characteristics of the natural boxfish (as shown in Fig. 1), which includes that (i) it generates gait transition while its swimming speed varies, i.e., the fish swims with paired and medium fins (two pectoral fins, one dorsal fin and one anal fin) at low speed and propels only with caudal fin at high speed; (ii) the speed of fish increases almost linearly with frequency and amplitude; (iii) the caudal fin has systematically lower frequency than the pectoral fins; (iv) the fish can produce multiple swimming modes. To validate the CPG model, we apply it to control a well designed boxfish robot with two pectoral fins and one caudal fin. Moreover, we design a CPG-based control architecture for the robot with sensory inputs provided by a vision sensor (camera) and an Inertial Measurement Unit (IMU).

This work was supported by grants from the National Natural Science Foundation of China (NSFC, No. 60774089, 10972003).

[1]W. Wang and [1]G. Xie are with the Intelligent Control Laboratory, College of Engineering, Peking University, Beijing 100871, China wangweiw4y4@pku.edu.cn; xiegming@pku.edu.cn

[2]J. Guo is with the School of Mechanical Science and Engineering, Huazhong University of Science and Technology, Wuhan 430074, China jiajie.guo@mail.hust.edu.cn

[3]Z. Wang is with the School of Automation Science and Electrical Engineering, Beihang University, Beijing 100191, China zijian.wang1991@gmail.com

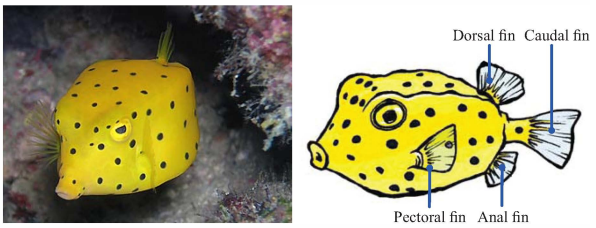

Fig. 1. Physiological structure of boxfish. (a) Yellow-spotted boxfish. (The picture is cited at http://www.chinadiver.com/wiki.) (b) Fins distribution of boxfish.

The rest of this paper is organized as follows: Section II describes the hardware of the robot. The novel CPG model for the ostraciiform robot is presented in Section III. Section IV illustrates the CPG-based control architecture. Experiments are provided in Section V to validate the proposed CPG model. Conclusion and future work are given at the end of this paper.

II. Hardware of Boxfish Robot

A. Mechanical Design

Fig. 2(a) shows mechanical configurations of the boxfish robot, which consist of a roughly rectangular main body, a pair of pectoral fins and a caudal fin. The rigid and waterproof main body housing rechargeable batteries, sensors and actuators, is composed of one upper transparent fiber reinforce plastic (FRP) shell and another lower lightened polyurethane shell. The fins are individually actuated by three Hitec servomotors, which have a maximum torque of 9.4 Kg·cm at 6 V. The two pectoral fins provide thrust for multimodal swimming while the caudal fin can acquire high swimming speed or act as a rudder. Both static and moving seals are adopted to ensure waterproof of the robot. Specifically, tailor-made O-rings and silicone adhesives are used between two external casings, while seal rings are used between driving shaft and body frames.

The rotation range of pectoral fins are $\pm 180^\circ$ by using the specially designed gear sets with a reduction ratio $2:1$, while motion range of the caudal fin is limited to $\pm 60^\circ$. All these three replaceable fins are made of PE plates with non-uniform thickness to approximate hardness and flexibility of the natural fins. Density of the robot has been calibrated close to water so that it can easily float in the water. By placing proper clump weight, mass distribution of the robot is well balanced in the tested position to achieve smooth 3D motions.

B. Electronics and sensors

Fig. 2(b) shows electronics and sensors in the robot. The main controller is Samsung S3C2440A microcontroller, which incorporates a 32-bit RISC, ARM920T CPU core and runs steadily at 400Mhz. Extended 64MB SDRAM and 64MB Nand Flash are used for high requirement of program execution and code storage. The controller board is developed independently at the Intelligent Control Laboratory at Peking University.

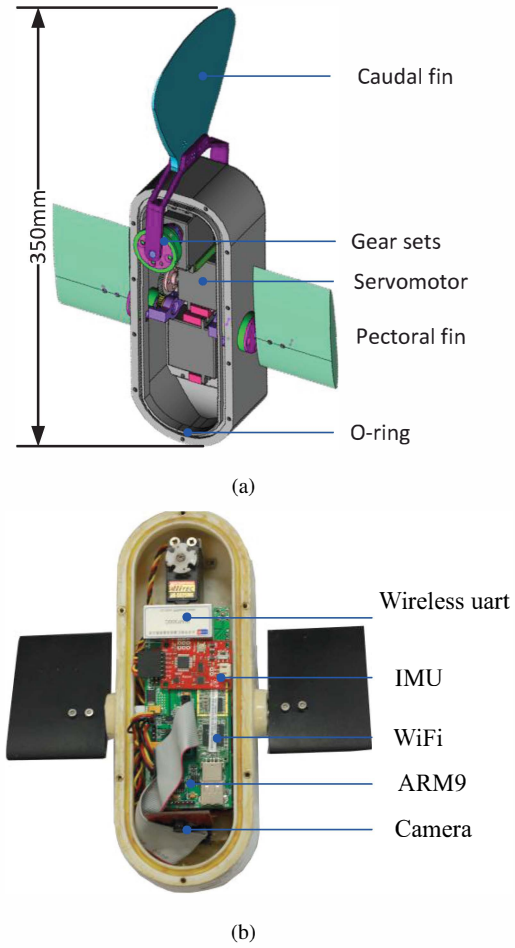

Fig. 2. Mechatronics of the boxfish robot. (a) Mechanical configuration of the robot. (b) Electronics and sensors in the robot.

A vision sensor OV9653 with 1.3 million pixels is placed centrally in the front of the main body. It captures images of surroundings for obstacle avoiding and localization. An IMU consisting of a triaxial gyroscope, a triaxial accelerometer and a triaxial electronic compass, is fixed parallel to the body principal axis. It acquires the robot's pitch, yaw and roll angles and can also measure accelerations of the robot for future developments. The sampling rate is set at 50 Hz for real-time application. The robot is operated by an embedded Linux system and state of it is monitored by a Windows server. Via wireless communication network (WiFi), the server can acquire underwater surroundings of the robot when it is near surface of the water.

III. Central Pattern Generator

This section proposes a novel CPG model to emulate its biological counterpart for producing multiple swimming modes and smooth swimming gait transition with only two simple input drives.

A. Three-layer CPG Model

As shown in Fig. 3, the CPG model consists of three functional layers, namely input saturation functions, coupled neural oscillators and output transition function. The

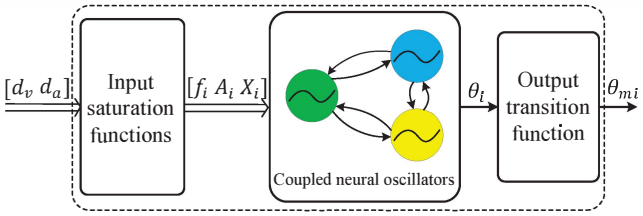

Fig. 3. The proposed three-layer CPG model.

input saturation function receives command signals from brainstem-like command centers for initiating, regulating and stopping CPG. The command d_v determines speed and gait transition of the robot by employing two input saturation functions, the command d_a determines the multiple swimming modes such as swimming forwards, turning and rolling. There are N coupled oscillators, functionally similar to the spinal cord in a biological neural system, which generates rhythmic motor patterns. The parameters f_i, A_i and X_i are frequency, amplitude, and offsets of the i^{th} oscillator, respectively. Analogous to muscles reacting to neural signals, output transition function translates the oscillation network output θ_i to the motor driving signal θ_{mi}.

Details of the saturation functions g_{fi}, g_{Ai} and g_{Xi} are given as follows:

$$f_i = g_{fi}(d_v) = \begin{cases} c_{fi} d_v + f_{i,b}, & \text{if } d_v^{i,\min} \le d_v \le d_v^{i,\max}; \\ f_{i,sat}, & \text{otherwise.} \end{cases} \tag{1}$$

$$A_i = g_{Ai}(d_v) = \begin{cases} c_{Ai} d_v + A_{i,b}, & \text{if } d_v^{i,\min} \le d_v \le d_v^{i,\max}; \\ A_{i,sat}, & \text{otherwise.} \end{cases} \tag{2}$$

$$X_1 = g_{X1}(d_a) = \begin{cases} \pi d_a & \text{if } d_a \in \{-\frac{1}{2}, \frac{1}{2}\} \\ 0, & \text{otherwise.} \end{cases} \tag{3a}$$

$$X_2 = g_{X2}(d_a) = \begin{cases} \pi(d_a - sgn(d_a)) & \text{if } d_a \in \{-\frac{1}{2}, \frac{1}{2}\} \\ 0, & \text{otherwise.} \end{cases} \tag{3b}$$

$$X_3 = g_{X3}(d_a) = \begin{cases} \pi d_a & \text{if} -\frac{1}{3} \le d_a \le \frac{1}{3} \\ 0, & \text{otherwise.} \end{cases} \tag{3c}$$

where $d_v^{i,\min}$ and $d_v^{i,\max}$ represent the lower and upper threshold drive d_v of the i^{th} oscillator, respectively; coefficients (c_{fi}, c_{Ai}), biases ($f_{i,b}$, $A_{i,b}$), and saturations ($f_{i,sat}$, $A_{i,sat}$) are used for modulating frequency and amplitude of the i^{th} oscillator, respectively.

It is desired that the proposed CPG model is robust and exhibits limit cycle behavior which enables the system to rapidly return to a steady state when subjected to small transient perturbations. For this purpose, the coupled neural oscillators are designed with the following forms as

$$\ddot{a}_i = \alpha\left(\alpha(A_i - a_i) - 2\dot{a}_i\right) \tag{4a}$$

$$\ddot{x}_i = \beta\left(\beta(X_i - x_i) - 2\dot{x}_i\right) \tag{4b}$$

$$\ddot{\phi}_i = \sum_{j=1, j\neq i}^{N} \mu_{ij}\left(\mu_{ij} a_j(\phi_j - \phi_i) - 2(\dot{\phi}_i - 2\pi f_i)\right) \tag{4c}$$

$$\theta_i = x_i + a_i \cos(\phi_i) \tag{4d}$$

where a_i, x_i, and ϕ_i are state variables representing amplitude, offset, and phase of the i^{th} oscillator, and variable θ_i is its output. The parameters f_i, A_i, and X_i are control parameters for the desired frequency, amplitude and offset of oscillations. The coupling effects among oscillators are determined by the coupling weights μ_{ij}. α and β are constant positive gains. Thus it can be seen that $a_i \to A_i$, $x_i \to X_i$ as the system approaches the steady state where $\ddot{a}_i = 0$, $\dot{a}_i = 0$, $\ddot{x}_i = 0$ and $\dot{x}_i = 0$. Note that f_i will eventually converge to the same frequency because of coupling effects among oscillators in spite that the oscillators have different intrinsic frequencies. We set all $f_i = f$ in the paper.

The third layer is output transition function $h_i(\theta_i)$ which translates the rhythmic neural oscillator signal to the motor actuating signal. It takes the form

$$\theta_m^i = h_i(\theta_i) = \begin{cases} \theta_m^{i,\max}, & \theta_i > \theta_i^{\max} \\ c_{mi}\theta_i + \theta_m^{bi}, & \theta_i^{\min} \le \theta_i \le \theta_i^{\max} \\ \theta_m^{i,\min}, & \theta_i < \theta_i^{\min} \end{cases} \tag{5}$$

where θ_m^i is the driving signal fed to corresponding servomotor; θ_m^{bi} is potential signal when the i^{th} servomotor stays at reference position and c_{mi} is the translation coefficient.

The values of constant parameter used throughout the paper are$(d_v^{1,\min}, d_v^{1,\max}, d_v^{2,\min}, d_v^{2,\max}, d_v^{3,\min}, d_v^{3,\max})$ = (1, 3, 1, 3, 3, 5); $\alpha = \beta = 20$ [rad/s] and $\mu_{ij} = 100$ [1/s] except $\mu_{11} = \mu_{22} = \mu_{33} = 0.0$ [1/s]; $c_{mi} = 1/180$, $(\theta_i^{\min}, \theta_i^{\max}) = (-180^\circ, 180^\circ)$ and $\theta_m^{bi} = 1.5$ ms; $i, j = 1, 2, 3$ represent the left-pectoral, right-pectoral and caudal fin, respectively.

For a given group of input parameters A_i under one frequency f, the CPG can produce rhythmic motion for the robot. However, it is insensible that whether the selected group of parameters is the best state (for example, it can produce fastest speed) for the certain frequency. Therefore, we conducted a large number of experiments for speed measurement with different combinations of amplitudes for certain beat frequencies with 0.25 Hz each step. From the experiments data, it is found that (i) higher frequency with relatively large amplitudes produces faster speed; (ii) however, higher amplitudes ($A_1 = A_2 > 30^\circ$, $A_3 > 30^\circ$) will not obtain faster speed for a given swimming frequency. For simplicity while without loss of accuracy, we suppose frequency and amplitude of each fin is linear with the input drive d_v, which has been defined in Eqn. 1 and 2. Therefore, the related parameters can be obtained as follows: $(A_{1,b}, A_{2,b}, A_{3,b}) = (7.5^\circ, 7.5^\circ, -7.5^\circ)$, $A_{i,sat} = 0^\circ$, $c_{Ai} = 7.5$, $(f_{1,b}, f_{2,b}, f_{3,b})$ = (0 Hz, 0 Hz, -0.8 Hz, $f_{i,sat}$ = 0 Hz, $(c_{f1}, c_{f2}, c_{f3}) =$ (1.4, 1.4, 0.8).

B. Model Analysis

Here we stress the explication that how drive d_v enables automatic gait transition between pectoral and caudal gait and that how drive d_a produces different swimming modes. In the CPG model, the pectoral and caudal gait exist exclusively to each other with bidirectional couplings among oscillation networks. At a low swimming speed, boxfish employs the pectoral gait which primarily oscillates two pectoral fins and keeps caudal fin stationary as a rudder, performing labriform swimming with considerable stability and maneuverability. At a high speed, boxfish employs the caudal gait by performing ostraciiform swimming to suppress the motions of pectoral fin and propels itself using only caudal fin as the primary thruster.

To analyze and simulate performance of the proposed model, we consider the fish-like robot with two pectoral fins and one caudal fin, and Fig. 4 shows that as input drive d_v increases, the model transits from the pectoral gait to caudal gait. When d_v is less than the lower threshold of pectoral oscillators ($d_v^{1,\min} = d_v^{2,\min}$), there is no oscillations in θ_i's. When d_v exceeds the lower threshold of the pectoral oscillators, the pectoral swimming gait is in action, during which the frequency f_i, amplitude A_i of the pectoral oscillators increase proportionally with d_v. When the pectoral oscillators saturate with d_v (exceeding the upper threshold of the pectoral oscillators ($d_v^{1,\max} = d_v^{2,\max} = d_v^{3,\min}$), the robot rapidly transits to the caudal gait with lower frequency but higher speed. As the input signal d_v further increases, the frequency and amplitude of caudal oscillator increase until the oscillator reaches its upper threshold ($d_v^{3,\max}$) and the robot stops.

Next, input d_a can enable multiple swimming modes and is analyzed as follows: when $d_a = 0$, all offsets (that is, X_i) of three fins are zero and the robot performs forward swimming; when $-\frac{\pi}{3} \le d_a \le \frac{\pi}{3}$, the robot begins to turn and when $d_a = -\frac{1}{2}$ or $d_a = \frac{1}{2}$, the robot produces rolling motion about its principal axis. Based on the analysis above, the proposed model has duplicated all the four characteristics (described in Section I) of a real boxfish.

IV. CPG-BASED CONTROL STRUCTURE

Based on the CPG model, the control architecture for the robot is shown in Fig. 5. Several swimming tasks such as target tracking and obstacle avoidance are designed and wirelessly sent to the robot from upper monitor platform. After receiving a task from the server, it analyzes sensory feedback from onboard camera and IMU, then outputs the drive signals into the CPG. Finally, properly calculated PWM signal actuates servomotor to produce periodic sinusoidal waveform, and further enables the robot to realize certain swimming patterns in the water.

Default task of the robot is target tracking which validates multiple swimming modes and two basic swimming gaits in different situations. Specifically, by regulating its swimming gaits, speed and direction, the robot can track a manually

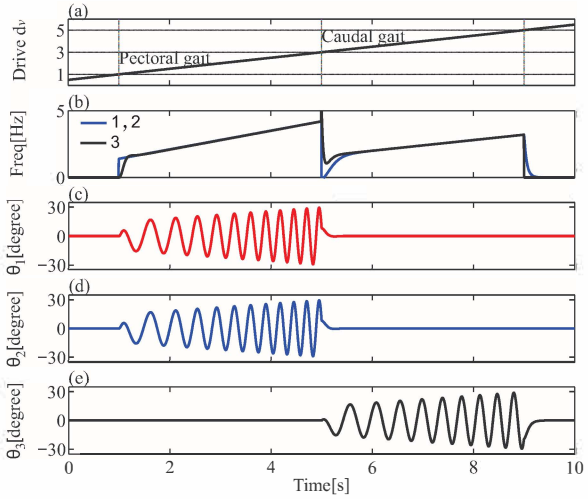

Fig. 4. Switching from pectoral gait to caudal gait as the drive signal d_v is progressively increased, while remains d_a = 0. (a) Linear increase of the drive d_v applied to all oscillators. (b) Instantaneous frequencies measured as $\frac{\dot{\theta}_i}{2\pi}$. (c) (d) (e) are oscillations corresponding to θ_1, θ_2 and θ_3, respectively.

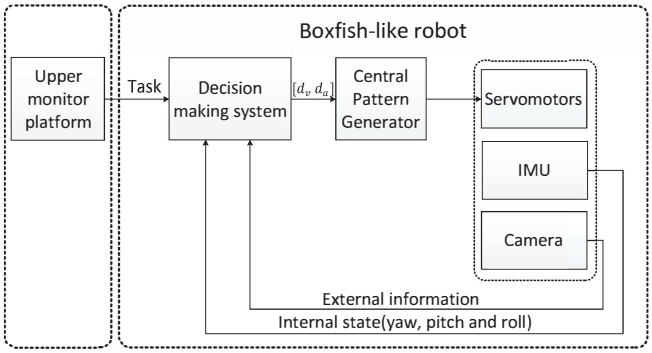

Fig. 5. Diagram of the complete control architecture for boxfish-like robot.

moving red ball at a constant distance (45 cm) while maintains the ball stationary in the center of its visual field. Details of adopted image processing method can be found in [16]. Making use of distance error e_λ between the robot and red ball and angle error e_ξ between horizontal principal axis of the robot and the line connecting center of the ball and center of camera, the CPG-based feedback control strategies are adopted as follows: (S1) when the distance error is small (-30 cm$\le e_\lambda \le$30 cm), the robot uses the pectoral gait to adjust. (S2) when the distance is too far away ($e_\lambda < -30$ cm), the robot switches to the caudal gait to speed up quickly. (S3) when the red ball is out of vision ($e_\lambda = \infty, e_\xi = \infty$), the robot turns according to its last distance value and offset angle. Details of above strategies are listed in Table I for different scenarios. The parameters k_1, k_2 and k_ξ are gains of the regulator; d_v^{last} and d_a^{last} are command values when the red ball is out of sight. Values of parameters in target tracking are $d_v^{c1} = 1.5$, $k_1 = 1/60$, $d_v^{c2} = 3.2$, $k_2 = 1/75$ and $k_\xi = 1$.

TABLE I

CONTROL LAW OF THE TRACKING SCENARIOS

Tracking scenarios	$S1$	$S2$	$S3$
d_v	$d_v^{c1} - k_1 e_\lambda$	$d_v^{c2} - k_2 e_\lambda$	d_v^{last}
d_a	$k_\xi e_\xi$	$k_\xi e_\xi$	d_a^{last}

V. RESULTS

A. Multiple Swimming Modes and Gait Transition

Various locomotion behaviors are obtained by abruptly changing inputs d_v and d_a. It is noted that output signals θ_i's of CPGs are continuous and smooth while the control commands are abruptly modified.

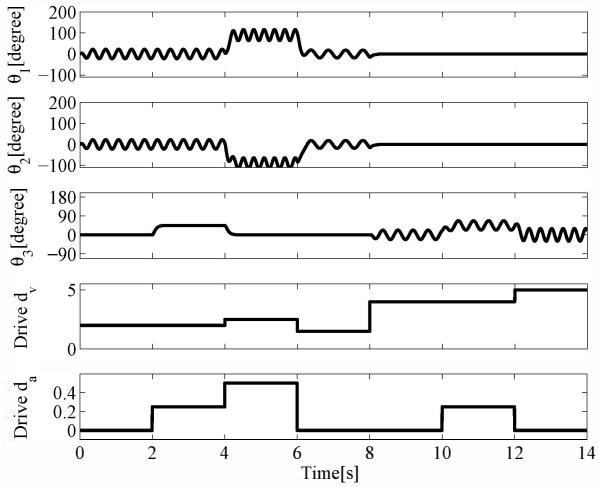

Fig. 6. Locomotion transitions involving two basic swimming gaits and multimodal swimming.

Fig. 6 demonstrates a sequence of swimming modes from one to another involving two basic swimming gaits. In the sequence, the transitions are organized as follows. (1) Swimming modes under the pectoral gait: swimming forwards with both pectorals ($0 \leq t \leq 2$ s), turning with the caudal offset ($2 \leq t \leq 4$ s), rolling ($4 \leq t \leq 6$ s) and slow swimming straight ($6 \leq t \leq 8$ s). (2) Swimming modes under the caudal gait: swimming forwards with caudal fins ($8 \leq t \leq 10$ s), turning ($10 \leq t \leq 12$ s) and fast swimming straight ($12 \leq t \leq 14$ s). Fig. 7 demonstrates maneuverability of the robot turning with caudal gait. Fig. 8 shows that the robot rolls using the pectoral fins. We can see that it is able to smoothly and rapidly transit among different swimming modes and switch between pectoral and caudal gaits. Therefore, similar to its natural counterpart, the robot realizes multiple swimming modes and speed-induced gait transition online under control of the proposed CPG model.

B. Speed Evaluation

Speed experiments were carried out to test characteristics of natural boxfish on the robot. Steady state speed was

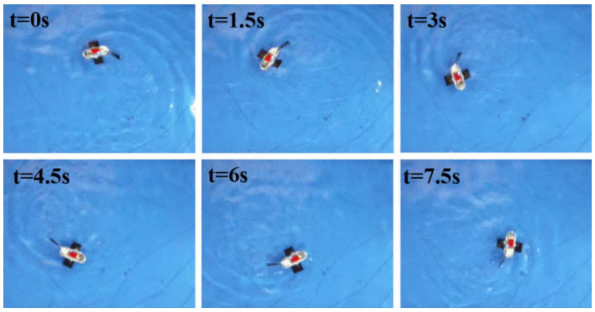

Fig. 7. The robot turns using the caudal gait. The drive signal d_v = 4 and $d_a = 0.25$.

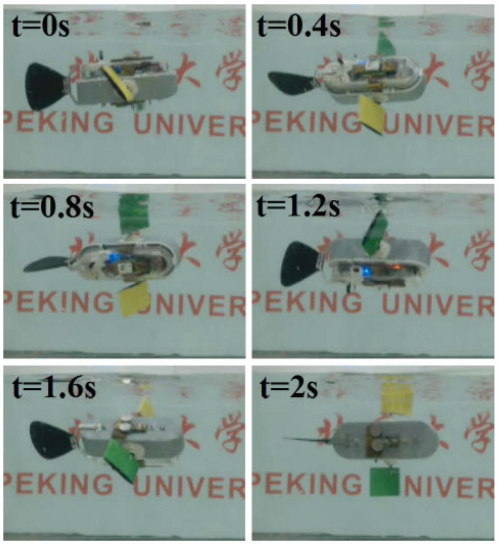

Fig. 8. The robot rolls with drive $d_v = 2.5$ and $d_a = -0.5$.

measured at various input signal d_v, as illustrated in Fig. 9. Swimming speed of the robot increases almost linearly with drive d_v. Given linear relation in Eqn. 1 and 2 between d_v and (f_i,A_i), it verifies the natural characteristic (ii) that swimming speed is positively proportional to beating frequency and amplitudes. Meanwhile, the robot can swim using two swimming gaits, and the caudal gait has a relatively higher speed than that of pectoral gait, which is consistent with natural characteristic (i). Overall, the robot can swim up to 0.21 m/s (0.60 BL/s) using the pectoral gait at a frequency of 4.2 Hz and amplitudes of $\pm 30^\circ$ while it reaches the highest speed of 0.38 m/s (1.09 BL/s) with the caudal gait at a frequency of 3.2 Hz and amplitudes of $\pm 30^\circ$.

C. Target Tracking

With a vision sensor integrated in the CPG-based control, the boxfish robot exhibits diverse swimming modes, gait transition and its fast response to environmental stimuli by tracking a moving ball. Fig. 10 illustrates the snapshots of target tracking process. The robot may lose sight of the target when the speed of the speed changes suddenly (e.g., the red ball speed increases dramatically or stops unexpectedly), then, it has to turn by itself until the target comes into view again. This is because that the fuzzy control law is relatively

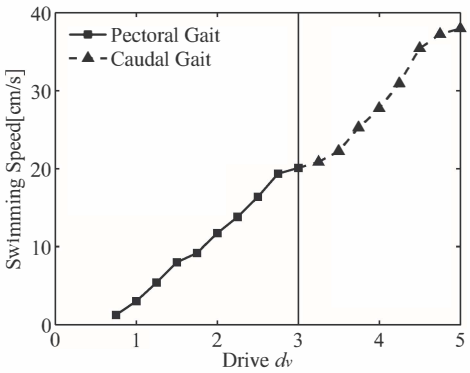

Fig. 9. Different forward swimming speed in term of varying input drive d_v under the basic two swimming gait, the offsets of the oscillators remains zero.

basic for choosing speeds and directions of the robot while the target speed is not considered in the control loop.

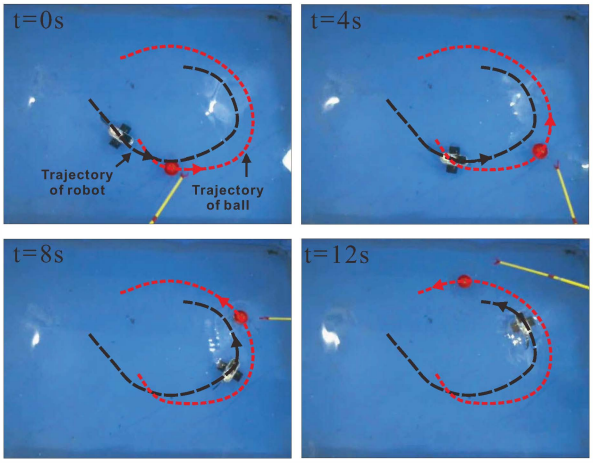

Fig. 10. Scenarios of target tracking experiment.

VI. Conclusion and Future Work

In this paper, a bio-inspired CPG model is proposed to control fish-like robots with multiple swimming modes (such as swimming forward, turning and rolling) and different swimming gaits by only two input drives. Its immediate application is illustrated by an ostraciiform fish robot with two pectoral fins and one caudal fin, which emulates its natural counterpart in four primary locomotion characteristics: (i) swimming gait transition, (ii) linear relation between speed and fin beating frequency/amplitude, (iii) intrinsic frequency of caudal gait lower than that of pectoral gait and (iv) multiple swimming modes. Similar to a biological neural system, the novel CPG-based control mechanism receives external stimuli, generates rhythmic and smooth neural signals and outputs drive signals to the actuators.

Drive d_a gives the robot great performance in flexibility and maneuverability in the 3D space while input d_v modulates the robot swimming between pectoral and caudal gaits with respect to the required speed. Moreover, target tracking was successfully performed to further validate the diverse swimming modes and gait transition under control of the CPG model. Therefore, the proposed model offers a promising approach for real-time control of swimming gait transition and multimodal swimming of the fish-like robot.

It is anticipated that the proposed CPG model will be a useful tool to investigate the swimming behaviors of natural fish. For this purpose, a general form of CPG model is needed to quantitatively control the robot's attitude (yaw, pitch and roll) with more simplified input drives. Other interesting topics like control parameters optimization, sensor network system and bio-inspired mechanical design are also worthy of further investigation.

References

[1] Y. Bar-Cohen, "Biomimetics-using nature to inspire human innovation," *Bioinspiration and Biomimetics*, vol. 1, no. 1, pp. 1–12, 2006.

[2] A. J. Ijspeert, "Central pattern generators for locomotion control in animals and robots: A review," *Neural Networks*, vol. 21, no. 4, pp. 642–653, 2008.

[3] F. Delcomyn, "Neural basis of rhythmic behavior in animals," *Science*, vol. 210, no. 4469, pp. 492–498, 1980.

[4] Y. Fukuoka, H. Kimura, and A. Cohen, "Adaptive dynamic walking of a quadruped robot on irregular terrain based on biological concepts," *The International Journal of Robotics Research*, vol. 22, no. 3-4, pp. 187–202, 2003.

[5] A. Crespi, A. Badertscher, A. Guignard, and A. Ijspeert, "Amphibot I: An amphibious snake-like robot," *Robotics and Autonomous Systems*, vol. 50, no. 4, pp. 163–175, 2005.

[6] W. Zhao, J. Yu, Y. Fang, and L. Wang, "Development of multimode biomimetic robotic fish based on central pattern generator," in *Proceedings of IEEE/RSJ International Conference, Intelligent Robots and Systems(IROS)*, 2006, pp. 3891–3896.

[7] A. Crespi and A. Ijspeert, "Amphibot II: An amphibious snake robot that crawls and swims using a central pattern generator," in *Proceedings of the 9th International Conference on Climbing and Walking Robots*, vol. 11, 2006, pp. 19–27.

[8] A. J. Ijspeert, A. Crespi, D. Ryczko, and J. M. Cabelguen, "From swimming to walking with a salamander robot driven by a spinal cord model," *Science*, vol. 315, no. 5817, pp. 1416–1420, 2007.

[9] J. Yu, R. Ding, Q. Yang, M. Tan, W. Wang, and J. Zhang, "On a bio-inspired amphibious robot capable of multimodal motion," *IEEE/ASME Trans. Mechatronics*, vol. 17, no. 5, pp. 847–856, 2012.

[10] J. Yu, M. Wang, M. Tan, and J. Zhang, "Three-dimensional swimming," *IEEE Trans. Robotics & Automation*, vol. 18, no. 4, pp. 47–58, 2011.

[11] A. Crespi, D. Lachat, A. Pasquier, and A. J. Ijspeert, "Controlling swimming and crawling in a fish robot using a central pattern generator," *Autonomous Robots*, vol. 25, no. 1-2, pp. 3–13, 2008.

[12] K. E. Korsmeyer, J. F. Steffensen, and J. Herskin, "Energetics of median and paired fin swimming, body and caudal fin swimming, and gait transition in parrotfish (scarus schlegeli) and triggerfish (rhinecanthus aculeatus)," *Journal of Experimental Biology*, vol. 205, no. 9, pp. 1253–1263, 2002.

[13] M. Wang, J. Yu, and M. Tan, "Modeling neural control of robotic fish with pectoral fins using a cpg-based network," in *Decision and Control, 2009 held jointly with the 2009 28th Chinese Control Conference. CDC/CCC 2009. Proceedings of the 48th IEEE Conference on*, dec. 2009, pp. 6502 –6507.

[14] Y. Hu, W. Zhao, L. Wang, and Y. Jia, "Neural-based control of modular robotic fish with multiple propulsors," in *Decision and Control, 2008. CDC 2008. 47th IEEE Conference on*, dec. 2008, pp. 5232 –5237.

[15] C. Wang, G. Xie, L. Wang, and M. Cao, "Cpg based locomotion control of a robotic fish: using linear oscillators and reducing control parameters via pso," *International Journal of Innovative Computing, Information and Control*, vol. 7, no. 7B, pp. 4237–4249, 2011.

[16] Y. Hu, W. Zhao, L. Wang, and Y. Jia, "Underwater target following with a vision-based autonomous robotic fish," in *Proceedings of IEEE International Conference, American Control Conference(ACC)*, 2009, pp. 5265–5270.